16th World Conference on Earthquake, 16WCEE 2017
Santiago Chile, January 9th to 13th 2017
Paper N° 2668 (Abstract ID)
Registration Code: S- Z1462783616

Response Characteristics of Operating Floor of Reactor Building in Onagawa Nuclear Power Plant Unit2 during Tohoku Earthquake 2011

K. Hirotani[1], Y. Ogata[2], Y. Ohashi[3], Y. Baba[4], O. Sugawara[5]

[1] *Deputy General Manager, Civil & Architectural Engineering Dept., Tohoku-Electric Power Co., Inc., hirotani.kiyoshi.nv@tohoku-epco.co.jp*
[2] *Manager, Civil & Architectural Engineering Dept., Tohoku-Electric Power Co., Inc., ogata.yoshihiro.kv@tohoku-epco.co.jp*
[3] *Manager, Nuclear Projects Division, Shimizu Corporation, ohashi_y@shimz.co.jp*
[4] *Nuclear Projects Division, Shimizu Corporation, yuka.b@shimz.co.jp*
[5] *Senior Manager, Structural Engineering, Nuclear Power Department, Kajima Corporation, sugawaos@kajima.com*

Abstract

The accelerometers recorded a maximum of 607 Gal and 1755 Gal on the basemat slab and roof slabs of the reactor building of Unit 2 of the Onagawa Nuclear Power Plant during the 2011 Tohoku Earthquake. In our previous paper [1], we confirmed the stiffness of the upper part of the operating floor was evidently degraded even though the reactor building maintained its structural integrity during the earthquake based on simulation analysis using lumped mass models.

In this paper, we perform additional simulation analysis by 3D-FEM in order to understand the behavior of the reactor building focusing on the material nonlinearity of the upper part of the shear walls during the earthquake. The initial stiffness of walls before the earthquake and the nonlinear material properties of concrete are calibrated with the seismic records and the simulation model.

The characteristics of the actual response of the operating floor were fully captured by the FEM model and as a result of the simulation the model numerically confirmed that the maximum strain values of the reinforcing bars were much smaller than the seismic capacity of shear walls during the earthquake.

Keywords: 3D-FEM; 2011 Tohoku Earthquake; Reinforced Concrete; Nuclear Power Plant

1. Introduction

The earthquake motion during the March 11, 2011 Tohoku Earthquake (hereafter “3/11”) were recorded on each floor of the reactor building of Unit 2 of the Onagawa Nuclear Power Plant (NPP). This plant is the closest nuclear power plant in Japan to the hypocenter. The maximum acceleration on the basemat slab and the top floor (roof) were 607 Gal and 1775 Gal respectively. In our previous paper [1], we simulated these observed responses by use of lumped mass models and concluded that the reactor building held its structural integrity during the earthquake even with stiffness degradation which was most significant on the upper part of the operating floor.

This article reports the result of nonlinear 3D-FEM simulation performed for the purpose of further investigation making use of the evaluation results of the structural soundness of the shear walls based on the simulation result. As the first step of the simulation, the initial stiffness of shear walls and tensile strength of concrete are calibrated. The initial stiffness of the walls is estimated from the relationship between relative story displacement and seismic force. The material properties of concrete are determined by pushover analysis with the finite element (FE) model of the shear walls. In the FEM analysis, nonlinear layered shell elements are employed to model the shear walls and roof slabs; and linear beam elements are used to model the steel columns, reinforced concrete girders, and steel trusses of the roof structure. The simulation analysis is also done for the lagest aftershock of 3/11 that occured on the April 7, 2011 (hereafter “4/07”).

2. Equivalent stiffness estimated from seismic record

2.1 Seismic record

As preparation for the dynamic simulation, we estimated the shear wall stiffness based on the seismic records of 3/11. To make the best use of the observed records, we used the relative story displacement records in addition to the acceleration records. The relative story displacement was directly measured by the measurement system on the operating floor, which was developed and installed before the Tohoku Earthquake by Tohoku Electric Power Company and Shimizu Corporation in order to obtain more precise measurements [2].

Observation points of acceleration on the operating floor and the roof are shown in Fig. 1. The measurement system of relative story displacement is illustrated in Fig. 2. Several acceleration time history records and relative story displacement records of 3/11 are shown in Fig. 3 and Fig. 4.

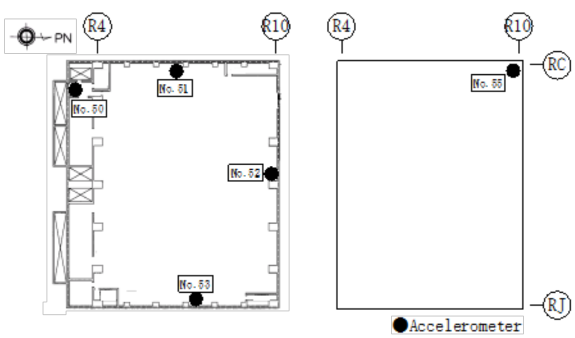

(a) Operating floor (b) Roof

Fig. 1 – Locations of accelerometers

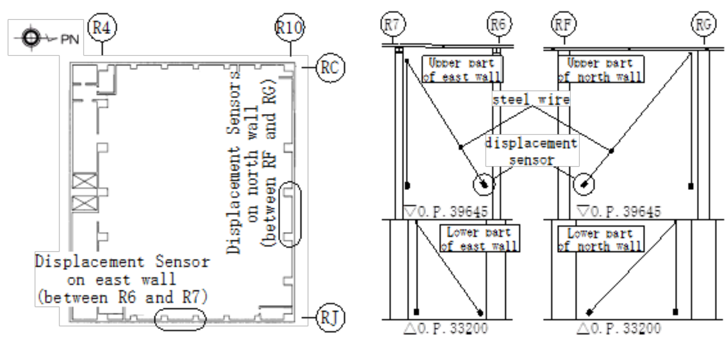

(a) Floor plan of operating floor (b) Wall extended elevation

Fig. 2 – Illustration of the measurement system of relative story displacement

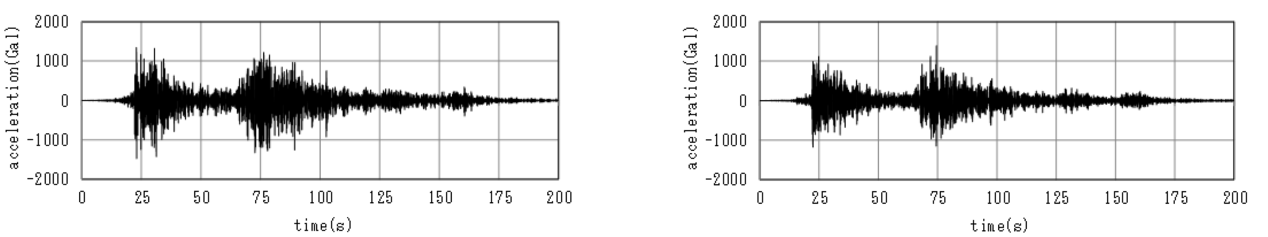

(a) NS direction (b) EW direction

Fig. 3 – Acceleration time history records on roof (3/11)

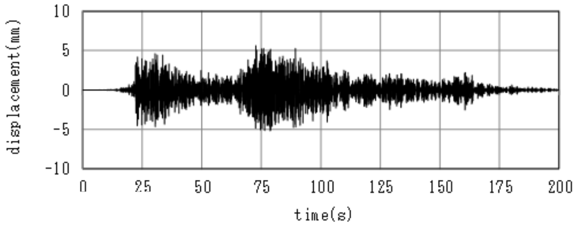

(a) Upper part of east wall

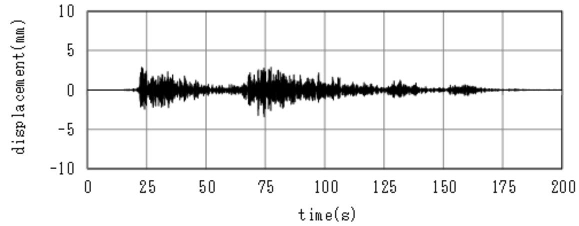

(b) Upper part of north wall

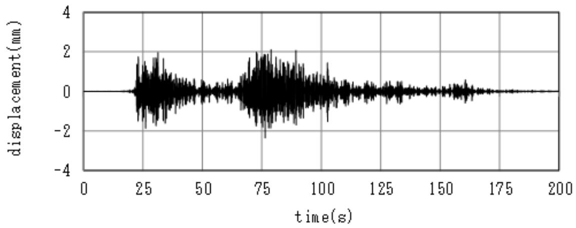

(c) Lower part of east wall

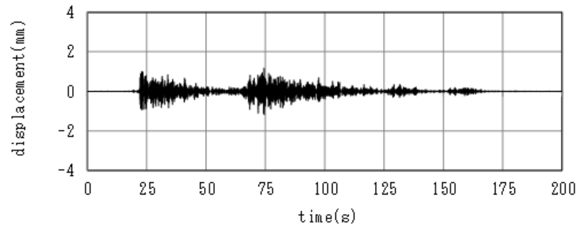

(d) Lower part of north wall

Fig. 4 – Relative story displacement time history records (3/11)

2.2 Method to estimate equivalent stiffness

When acceleration records on two floors are available, transfer function between them reasonably reflects the structural properties including stiffness. While the adopted method to estimate equivalent stiffness in this paper =is based on force-displacement relationship, since we have displacement records measured by the measurement system of relative story displacement. Seismic shear force is estimated by mass and acceleration records. The equivalent stiffness is calculated from relationship between seismic force and relative story displacement directly as per Eq. (1) as follows:

$$K_i = \frac{\sum_{j=1}^{n} \frac{R_{ij} \cdot Q_{ij}}{D_{ij}}}{\sum_{j=1}^{n} R_{ij}} \quad , \quad R_{ij} = \sqrt{{Q_{ij}}^2 + {D_{ij}}^2} \tag{1}$$

where K_i is stiffness of i-th loop, R_{ij} is weight factor, Q_{ij} is j-th force of i-th loop, n is the number of data in i-th loop, and D_{ij} is j-th relative story displacement of i-th loop. However, only the loops on the force-displacement plane satisfying the following conditions are extracted and used:

- Loops in the first quadrant or the third quadrant,
- Loops rotate clockwise around the origin.

The seismic force is calculated by multiplying the acceleration by lumped mass at the floor level. The relative story displacement is recorded directly by the measurement system. The force-displacement loops for 3/11 data are plotted in Fig. 5 and are compared with the elastic stiffness calculated by the FE model with linear material (detailed in Chapter 3). The time history records were band-pass filtered from 3.0 to 11.0Hz. The band range covers both the first mode natural frequency of the soil-structure interaction system of approximately 4.5Hz, and the first natural frequency of the upper structure above the operating floor of approximately 10.0Hz.

2.3 Estimated equivalent stiffness before the 3/11 Earthquake

The estimated equivalent stiffness of each loop is plotted in Fig. 6. The average stiffness of four portions of the motion is listed in Table 1 as follows: initial motion (19-22 sec), 1st strong motion (20-40 sec), 2nd strong motion (60-80 sec), and later arrival motion (80-100 sec).

Table 1 – Estimated equivalent stiffness (10^6 kN/m)

	Elastic stiffness	Average equivalent stiffness			
		19 – 22 sec	20 – 40 sec	60 – 80 sec	80 – 100 sec
Upper east wall	8.0	3.7 (0.5)	2.7 (0.3)	2.3 (0.3)	2.1 (0.3)
Lower east wall	38.0	42.0 (1.1)	16.7 (0.4)	13.9 (0.4)	10.7 (0.3)
Upper north wall	13.9	11.3 (0.8)	5.1 (0.4)	5.0 (0.4)	3.6 (0.3)
Lower north wall	46.5	54.1 (1.2)	20.5 (0.4)	20.5 (0.4)	18.7 (0.4)

* ( ) indicates ratio of estimated equivalent stiffness to elastic stiffness

The stiffness was evidently degraded during the 1st strong motions: 30 to 40 percent of the elastic stiffness. It is also noted that the initial stiffness during the initial motion is estimated lower than the elastic stiffness at the upper parts of the walls. The ratio of the elastic stiffness was estimated at 0.5 for the east wall and 0.8 for the north wall.

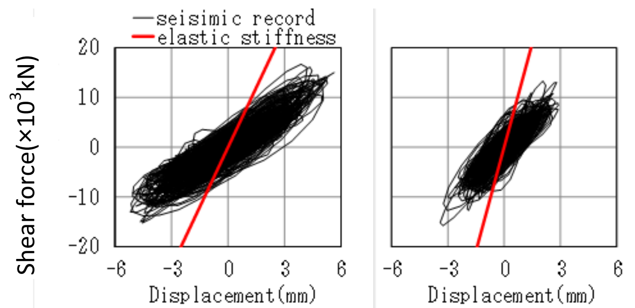

(a) Upper part of east wall (left)

and north wall (right)

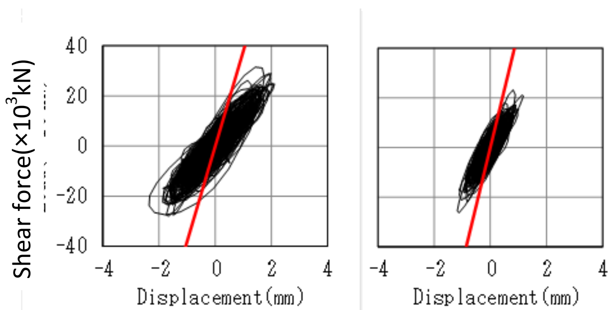

(b) Lower part of east wall (left)

and north wall (right)

Fig. 5 – Force-displacement curves

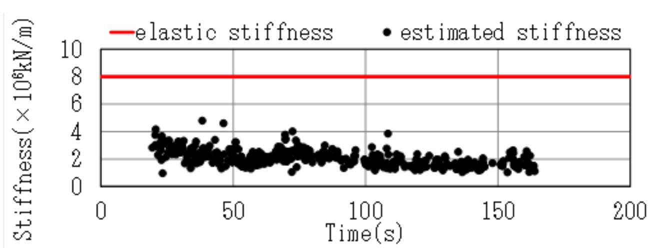

(a) Upper part of east wall

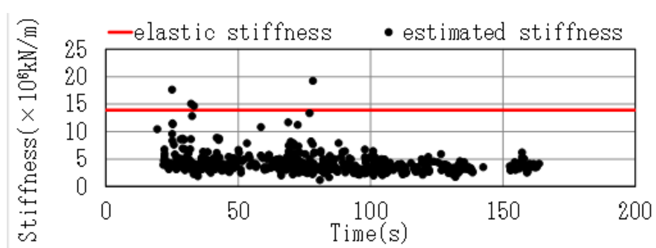

(b) Upper part of north wall

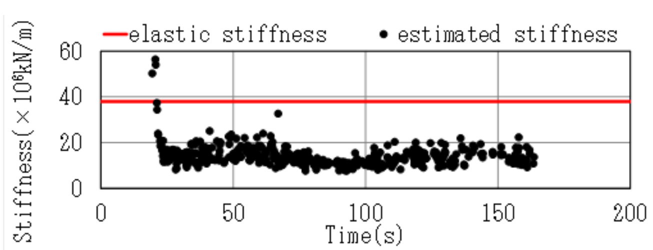

(c) Lower part of east wall

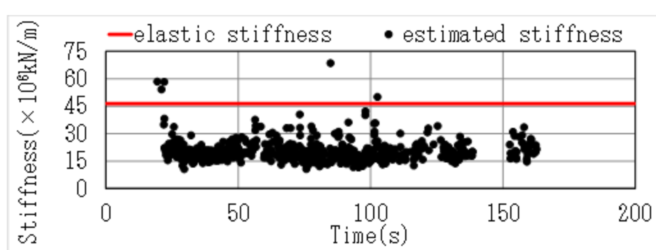

(d) Lower part of north wall

Fig. 6 – Estimated Stiffness

3. Study of concrete parameters by pushover analysis

The material parameters of concrete are determined by pushover analysis of the 3D FE models of the east and north shear walls with which both the maximum force and the maximum displacement during 3/11 are reproduced.

3.1 FE model of shear walls

The FE models of the east and north walls are shown in Fig. 7. Laminated shell element and smeared crack model [3] are used for the concrete shear walls. The laminated shell elements are divided into 7 layers in the thickness direction, and two layers including rebar are modeled as reinforced concrete. The other layers are plain concrete. The seismic force obtained in Chapter 2 is loaded beyond either the maximum relative story displacement of 3/11 with displacement control or the maximum force of 3/11 with force control.

The compressive strength F_c and the Young's modulus of concrete are 56.6 N/mm^2 and 3.34 x10^4 N/mm^2 respectively according to the core test. The stiffness ratio in Table 2 (the stiffness ratio in Table 1 was tuned for better fitting) is multiplied to the Young's modulus in the following analyses (Chapter 3 and 4) .And the compressive strength F_c is not changed.

We also control the tensile strength with the parameter “tensile strength ratio”, which is determined through the analysis. The tensile strength is calculated by multiplying the tensile strength ratio to the standard tensile strength f_t (Eq. 2).

$$f_t = 0.38\sqrt{F_c} = 2.86 N / mm^2 \tag{2}$$

Table 2 – Stiffness factor and tensile strength ratio

Case	East wall				North wall			
	Upper part		Lower part		Upper part		Lower part	
	Stiffness ratio	Tensile strength ratio	Stiffness ratio	Tensile strength ratio	Stiffness ratio	Tensile strength ratio	Stiffness ratio	Tensile strength ratio
1	0.6	1.0	1.0	1.0	0.8	1.0	1.0	1.0
2	0.6	0.4	1.0	0.4	0.8	0.2	1.0	0.2

3.2 Result of pushover analysis

The response of shear force and relative story displacement are shown in Fig. 8. The maximum displacement (circles) and the maximum force (triangles), that are based on the 3/11 observation, should be identical on the force-displacement plane but there are discrepancies between them. However, we found the gap in Case 2 is much smaller than that in Case 1.

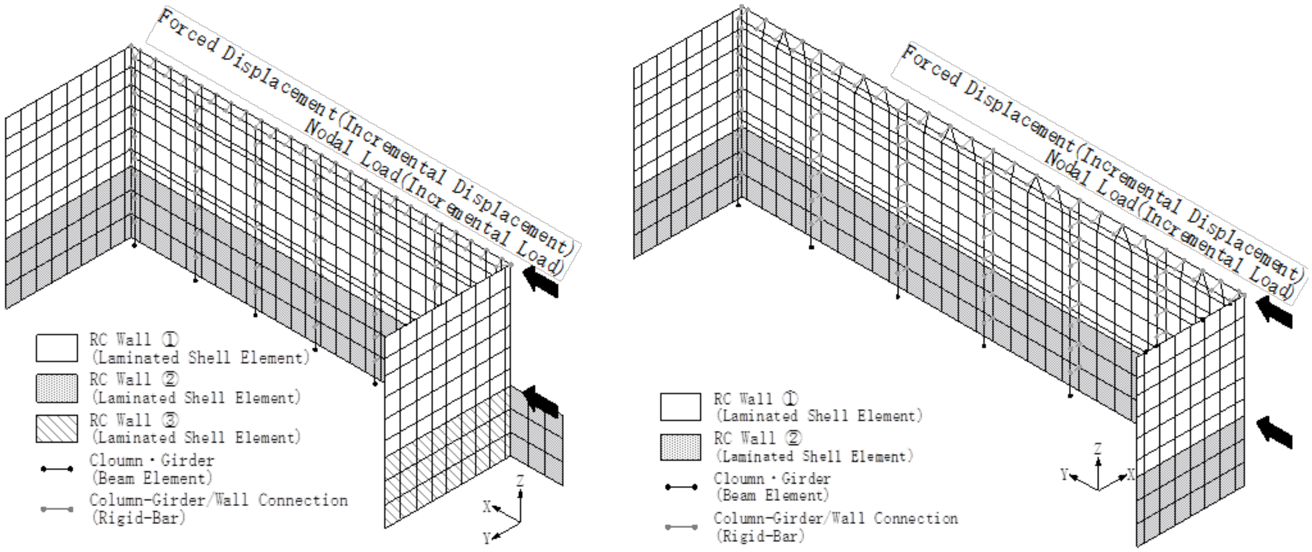

(a) East wall (b) North wall

Fig. 7 – FE models for pushover analysis

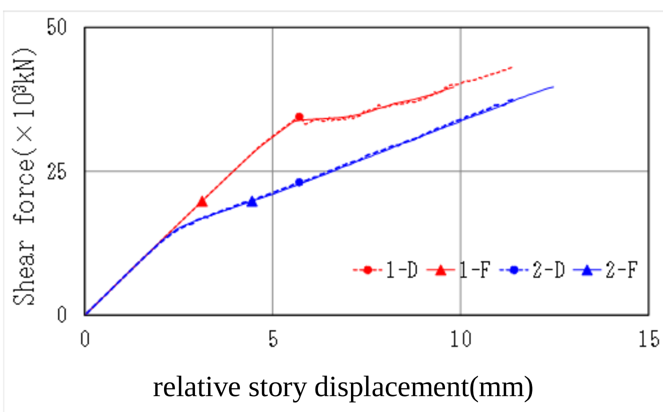

(a) Upper east wall

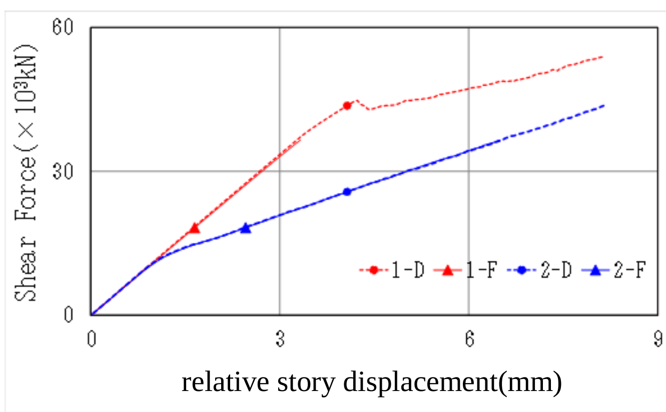

(b) Upper north wall

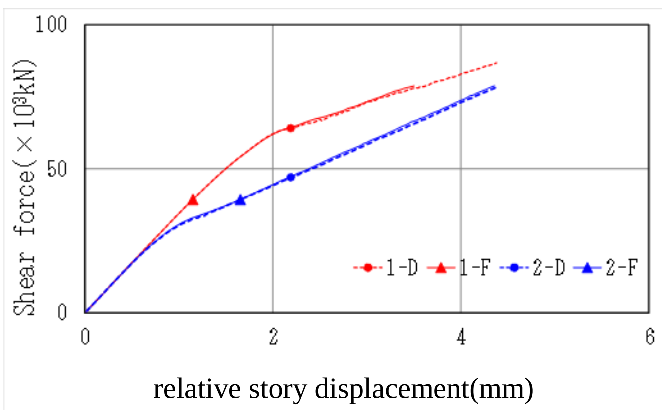

(c) Lower east wall

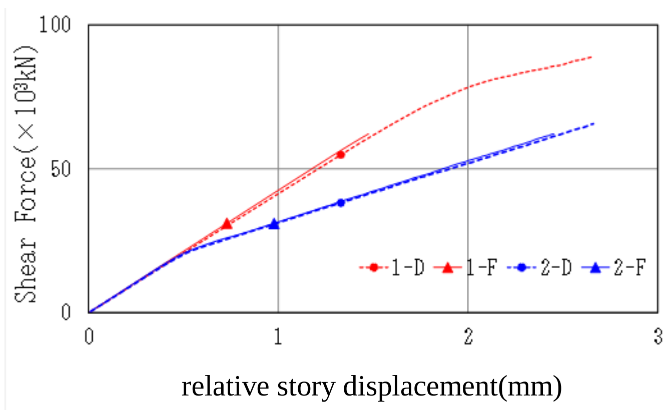

(d) Lower north wall

Fig. 8 – Shear force vs Relative story displacement (1-D/1-F: Case1 with displacement/force control, 2-D/2-F: Case 2 with displacement/force control, Circles: the maximum relative story displacement, triangles: the maximum force)

4. Simulation with FE model of upper structure

4.1 FE model of upper structure

The FE model for the upper structure above the operating floor was created as shown in Fig. 9. The shear walls and the top roof slab are modeled with a nonlinear constitutive material in the same manner as the FE model in the pushover analysis. The other elements; laminated shell elements as lower roof slab, beam elements as RC columns, steel beams, and truss, are all linear.

The weight of the upper structure is adjusted to the weight of the Multi-Degree-Of-Freedom model used in our previous paper [1] by increasing the density of the top slab and adding extra lumped masses to the nodes of columns and walls under the lower roof slab level where the cranes attach. Initial axial force is preloaded on each column as the gravity effect.

4.2 Input motions

All the nodes at the bottom of walls and columns on the operating floor are connected with rigid bars to a node specified as the center of gravity to impose input motions. The input motions have five components, except for the torsional component. The five components are imposed to the model simultaneously. The acceleration data observed at the accelerometers No. 51 in NS direction and No. 52 in EW direction in Fig. 1 is used for the two horizontal translational motions. The vertical records of No. 50, 51, 52 and 53 are converted to two rotational motions and one vertical motion at the center of gravity.

In this analysis, the imposed motions include both records of 3/11 and the 4/07 earthquakes consecutively combined as the translational motions shown in Fig. 10.

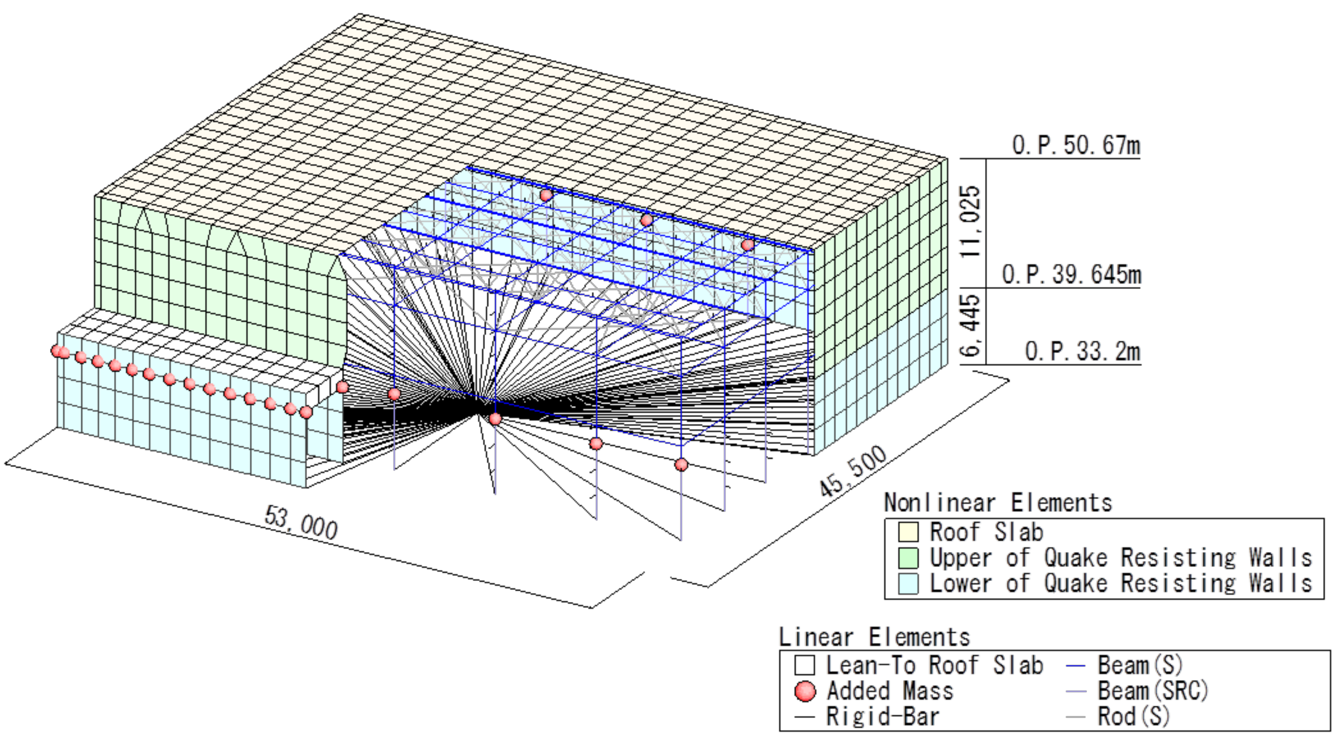

Fig. 9 – FE model of upper structure

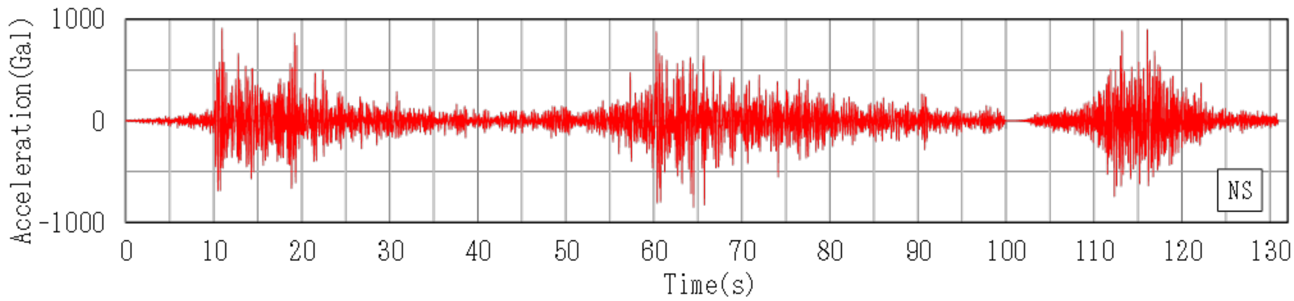

(a) NS direction

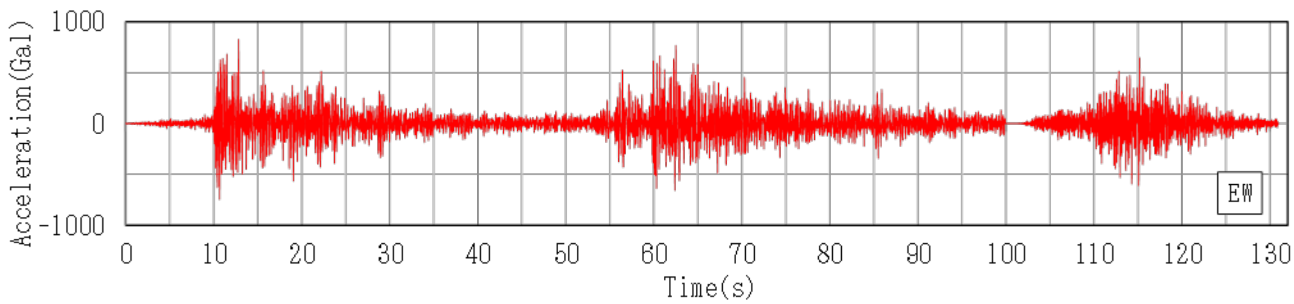

(b) EW direction

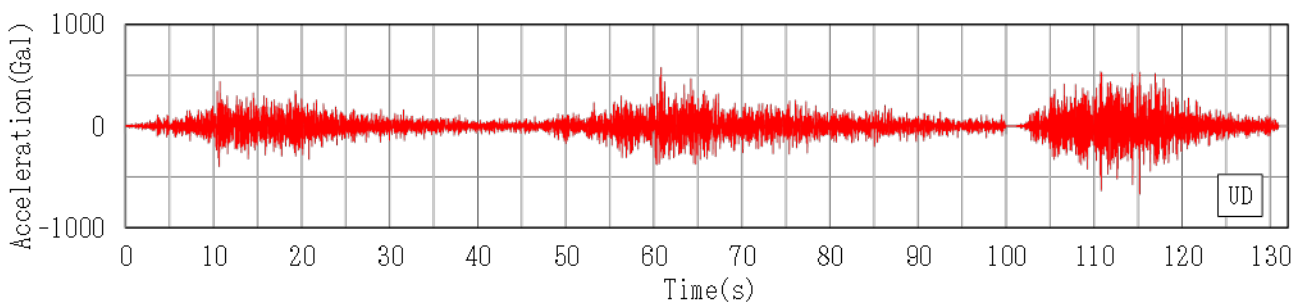

(c) UD direction

Fig. 10 – Translational input motions (until 100 sec: 3/11 records, after 30 sec: 4/07)

4.3 Material parameters

The concrete material parameters are set as well as the pushover analysis, and the stiffness ratio and tensile strength ratio of Case 1 and Case 2 in Table 2 are also used.

5. Result of dynamic simulation analysis

5.1 Acceleration response spectra

We compared the seismic record and the response of the node, whose location is near the accelerometer No.55 in Fig. 1. Comparison of acceleration response spectra is shown in Fig. 11 and Fig. 12. It was found that Case 2 gives a better fit to the observation in the period range over 0.1 sec. Case 2 could not reproduce well the peak around 0.2 sec in NS direction. As for the short period range less than 0.1 sec, the simulation tends to give larger response than the observation, and the spiky peak in UD direction of 3/11 was not reproduced in either case.

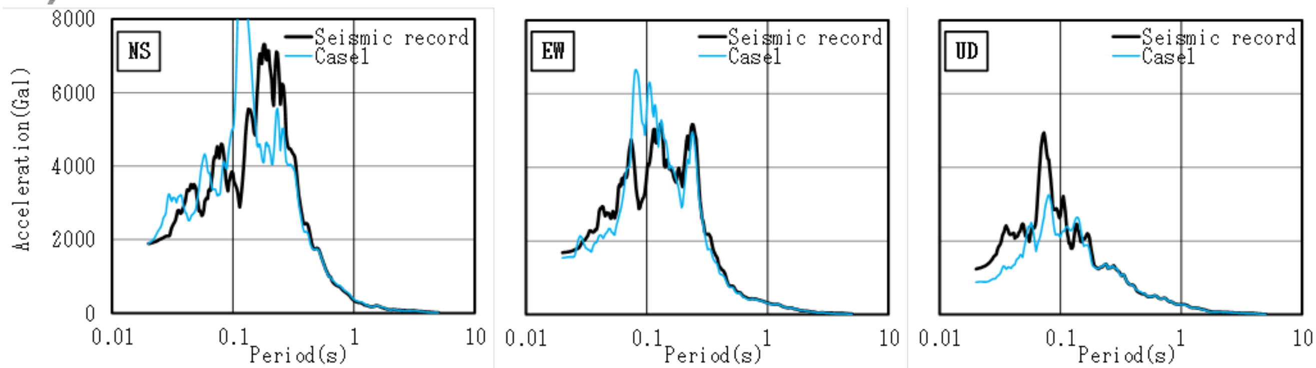

(a) Case1

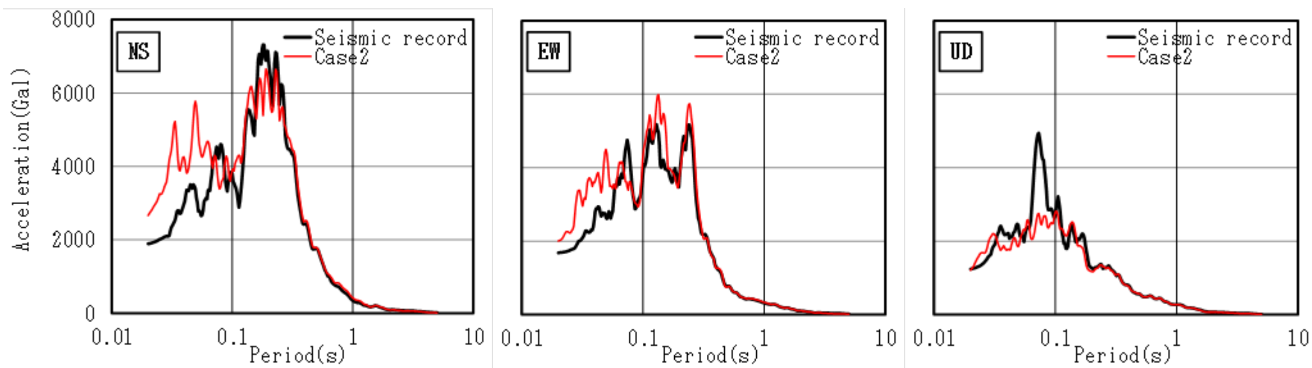

(b) Case2

Fig. 11 – Acceleration response spectra for floor response vs 3/11 seismic records

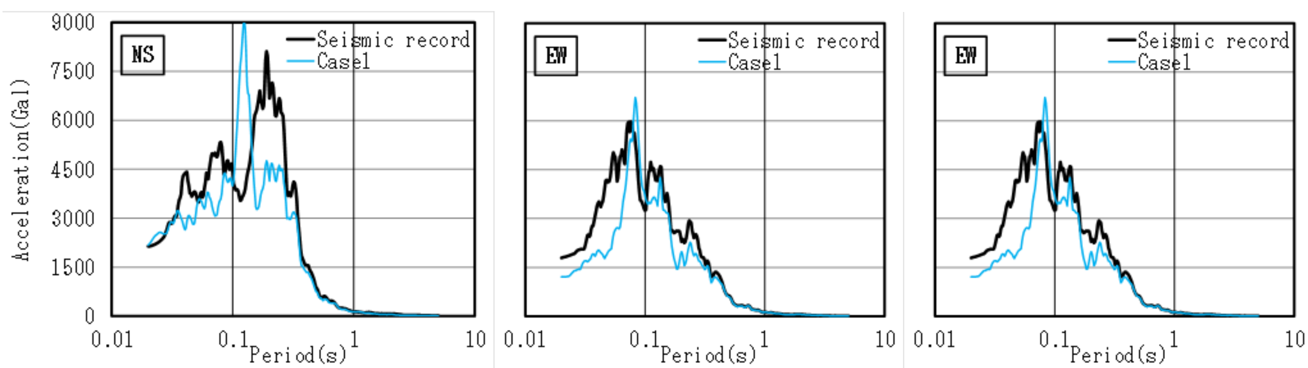

(a) Case1

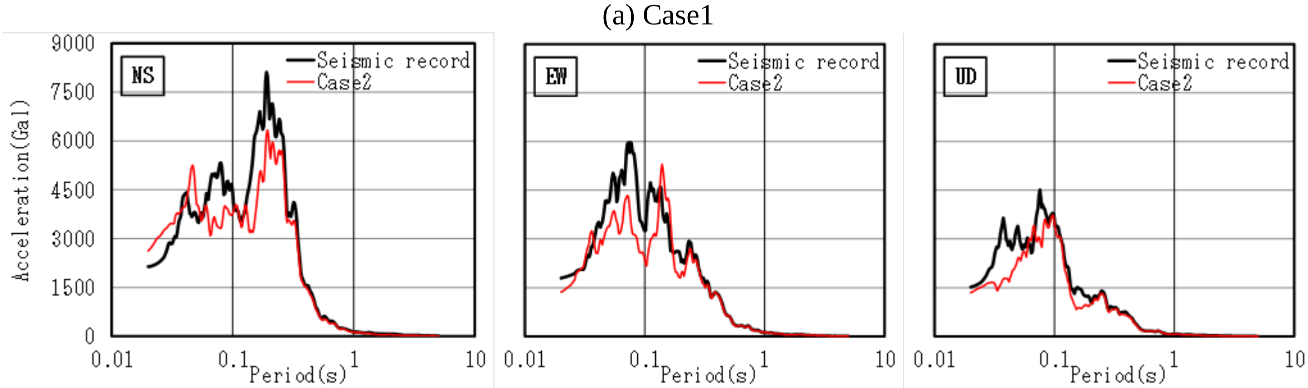

(b) Case2

Fig. 12 – Acceleration response spectra for floor response vs 4/07 seismic records

5.2 Strain of rebar in Case 2

Fig.13 shows maximum tensile strain distribution of rebar in the east and north wall. The value of maximum tensile strain was 676 μ for the horizontal rebar and 614 μ for the vertical rebar. The maximum tensile strain never exceeded the yield strain.

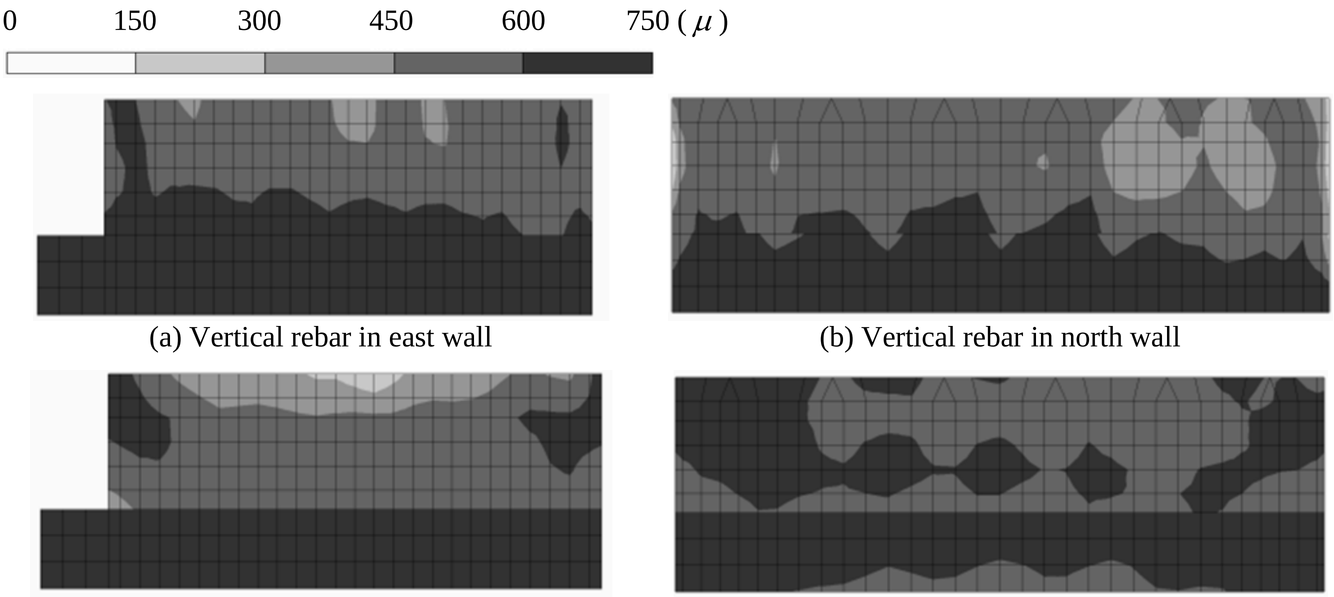

(a) Vertical rebar in east wall

(b) Vertical rebar in north wall

(c) Horizontal rebar in east wall

(c) Horizontal rebar in north wall

Fig. 13 – Maximum tensile strain of rebar in Case 2

6. Conclusion

The conclusion is summarized below:

The equivalent stiffness of walls above the operating floor was estimated based on the seismic records of 3/11. The tensile strength of concrete was specified through the pushover analysis. For both the equivalent stiffness and the tensile strength, the maximum force and relative story displacement in the pushover analysis were consistent with each other.

We simulated the seismic records on the top slab with the FE model in 3D in consideration of material nonlinearity of concrete. The characteristic of acceleration spectra in the period over 1.0 sec for the seismic records of both 3/11 and 4/07 are well reproduced with the equivalent stiffness and the tensile strength calibrated in the pushover analysis.

According to the maximum strain of rebar in the shear walls in the simulation, it was found out that the strain did not exceed the yield strain and the upper structure could maintain its structural integrity during the 3/11 and the 4/07 earthquakes.

7. References

[1] Hirotani K, Ogata Y, Otake H, Iida J (2012): Simulation Analysis of Earthquake Response of Onagawa Nuclear Power Plant the 2011 off the Pacific Coast of Tohoku Earthquake. *15th World Conference on Earthquake Engineering*

[2] Ogata Y, Sugawara Y, Ohtake H, Kurosawa I, Fujita Y, Inoue N (2011): Development of a Measurement System with Steel Wire for Relative Story Displacement. *Journal of Structural Engineering. B*, Vol.57B, 107-113,

[3] Maekawa K, Fukuura N (1999) : Re-Formulation of Spatially Averaged RC Constitutive Model with Quasi-Orthogonal Bi-Directional Cracking, *Journal of Japan Society of Civil Engineers*, No.634/V-45, 157-176